*Math. Model. Nat. Phenom.*
**Vol. 9, No. 1, 2014, pp. 58–81**
DOI: 10.1051/mmnp/20149204

# Pairwise and Edge-based Models of Epidemic Dynamics on Correlated Weighted Networks

P. Rattana[1], J.C. Miller[2], I.Z. Kiss[1] *

[1]School of Mathematical and Physical Sciences, Department of Mathematics
University of Sussex, Falmer, Brighton BN1 9QH, UK

[2]School of Mathematical Sciences, School of Biological Sciences, and the Monash Academy for Cross & Interdisciplinary Mathematics, Monash University, VIC 3800, Australia

**Abstract.** In this paper we explore the potential of the pairwise-type modelling approach to be extended to weighted networks where nodal degree and weights are not independent. As a baseline or null model for weighted networks, we consider undirected, heterogenous networks where edge weights are randomly distributed. We show that the pairwise model successfully captures the extra complexity of the network, but does this at the cost of limited analytical tractability due the high number of equations. To circumvent this problem, we employ the edge-based modelling approach to derive models corresponding to two different cases, namely for degree-dependent and randomly distributed weights. These models are more amenable to compute important epidemic descriptors, such as early growth rate and final epidemic size, and produce similarly excellent agreement with simulation. Using a branching process approach we compute the basic reproductive ratio for both models and discuss the implication of random and correlated weight distributions on this as well as on the time evolution and final outcome of epidemics. Finally, we illustrate that the two seemingly different modelling approaches, pairwise and edge-based, operate on similar assumptions and it is possible to formally link the two.

**Keywords and phrases:** weighted network, pairwise model, edge-based compartmental modelling, probability generating function

**Mathematics Subject Classification:** 05C82, 37N25, 91D30, 92D30

## 1. Introduction

The study of epidemic spread through contact networks has significantly improved our understanding of how the structure of interactions influences the spread of an infectious disease. One of the most recognised facts is that individuals with more contacts tend to become infected sooner and then spread the disease more quickly than others. Thus, for a given average degree, epidemics tend to spread faster if the population has a more heterogeneous degree distribution.

A number of models have been introduced to study the spread of an $SIR$ (susceptible-infectious-recovered) infectious disease through a class of random networks known as configuration model networks [19]. The earliest models [16] were restricted to final size calculations, predicting how the total number

*Corresponding author. E-mail: i.z.kiss@sussex.ac.uk

© EDP Sciences, 2014

Article published by EDP Sciences and available at http://www.mmnp-journal.org or http://dx.doi.org/10.1051/mmnp/20149204
https://doi.org/10.1051/mmnp/20149204 Published online by Cambridge University Press

infected depends on the transmission probability. More recently, models have been introduced which attempt to predict the dynamics of an epidemic, with varying levels of success and degrees of complexity. There are now several models available which can predict with high accuracy the population-scale dynamics of an $SIR$ epidemic spreading through a configuration model network [6, 9, 14, 18, 24].

However, these analyses assume that all interactions have the same strength. In fact some connections are expected to transmit infection quicker than others as a result of the closeness of interaction of the individuals. By itself, a heterogeneous distribution of contact weights would affect the dynamics of an epidemic. However, we further expect that an individual's contact-weights are likely to have some dependence on the degree of the nodes that the edges/links connect. Previous studies have considered and analysed different scenarios of weighted networks based on theoretical/synthetic network models [5, 15, 20, 22], as well as empirical networks reconstructed from real data (e.g. social mixing data [13] and cattle movements between farms [17]). These studies have typically focused on specific models that either gave information about (a) threshold quantities and final epidemic size, (b) mean-field type models for describing the time evolution of infection or (c) simulation. Here, we will aim to cover as many of these aspects as possible in one single body of work.

In this paper we develop and analyse models which allow us to incorporate edge-weights into the epidemic dynamics and we explore this via pairwise and edge-based compartmental models, as well as simulation. In particular, we focus on weighted networks where link or edge weights and node degree are not independent, see for example [8, 21]. The aim of this study is twofold. First, we explore the flexibility of the pairwise and edge-based compartmental modelling frameworks to account for this added level of complexity, and second, to gain better understanding on the precise impact of different weight distributions and of correlations between link-weight and degree on epidemic threshold, growth rate and epidemic dynamics. The paper is organised as follows. Section 2 is dedicated to model derivation starting with network construction and edge-weight distribution, including some null models, such as where link-weights are randomly distributed and where all link weights are equal to some predetermined average. In this same section, we derive and present the pairwise and edge-based models for random and degree-dependent weights cases. Section 3 is dedicated to results, and it is divided into analytic, numeric and model comparison parts. Finally, in section 4, we provide further aspects for discussion and future directions.

## 2. Model derivation

The models are built in a bottom up approach. We first describe the construction of the networks we study and how their edge-weights are assigned. We then describe the disease dynamics and simulation model. We conclude this section with the formulation and derivation of the pairwise and edge-based compartmental models for two distinct classes of weighted networks.

### 2.1. Network construction and simulation

Our focus here is the construction of our model networks and the simulation of an epidemic through those networks. Our model networks use the configuration model framework [19] with each edge assigned one of $M$ possible weights. The two network types we consider differ in how those weights are assigned to edges. We make standard assumptions about the disease spread, but we let the rate of transmission along an edge depend on its weight.

#### *2.1.1. Networks with randomly-distributed edge weights*

In this case a two step approach is used to generate networks with randomly-distributed edge weights. First, a network of $N$ nodes with prescribed degree distribution $P(k)$ is generated according to the configuration model. This procedure leads to an undirected unweighted network where edge weights can be now assigned at random according to a specified weight distribution $Q(w)$. If $Q(w)$ is defined across weights $w_i$, where $Q(w_i) = q_i$ and $i = 1, 2, \ldots, M$, then in a homogenous random network (i.e. all nodes have degree $k$), the distribution of edge-weights of various types is multinomial with parameters $k$



https://doi.org/10.1051/mmnp/20149204 Published online by Cambridge University Press

- number of trials and $q_i$ - the probability of a link being of weight $w_i$ with $i = 1, 2, \ldots, M$. The average weight in the network is given by $\langle w \rangle_{random} = \sum_{i=1}^{M} q_i w_i$.

While this is a good baseline model it is unlikely that this scenario would be a true representation of social interactions. For example, different weights could be interpreted as representing different social interactions (e.g. household, workplace and casual) and this could suggest a model where each individual has a certain number of links of different weights. Ignoring degree heterogeneity and considering individuals to be equal can result in a weighted network with fixed edge-weights, e.g. each node has $k$ links with $k_1$ being of household type and with $k_2 = k - k_1$ being of workplace type and thus of different weights, say $w_1$ and $w_2$ [20].

*2.1.2. Degree-dependent weighted networks*

While many different edge-weight allocation scenarios are possible, we opt to investigate the case where edge weights and node degrees are not independent. This is in contrast with the random edge weights case, where the network topology and the edge weight distribution and allocation are totally uncoupled. In particular, we wish to investigate an intuitively plausible idea which suggests that the weight or 'strength' of a link is negatively correlated to node-degree since individuals with many contacts are likely to afford a limited time commitment per link, and thus less of an opportunity for the disease to transmit [8,21]. In line with these studies, we propose a weighted network model where the link-weight between two nodes of degree $i$ and $j$, respectively, is given by $w(i,j) = w_{ij}$ with some functional form such that link-weight decreases as the degrees of nodes that it connects increase. Generating such a network is straightforward and it requires that first a configuration network with given degree distribution (i.e. $P(k)$) is created. This is followed by allocating weights to all links based on the degrees of the end nodes and according some pre-specified function $w(i,j)$, where $i, j = k_{min}, \ldots, k_{max}$ with $k_{min}$ and $k_{max}$ being the minimal and maximal nodal degree in the network. In this case, the distribution of weights is such that $Q(W = w(i,j)) = NP(i)i\frac{jP(j)}{\langle k \rangle}/(\langle k \rangle N/2) = \frac{2ijP(i)P(j)}{\langle k \rangle^2}$ and $Q(W = w(i,i)) = NP(i)i\frac{iP(i)}{\langle k \rangle}/(\langle k \rangle N) = \frac{i^2P^2(i)}{\langle k \rangle^2}$, where $W$ is the random variable corresponding to link-weights. Furthermore, discarding information about the degrees of the nodes for a link and simply assigning a random variable $W$ according to the distribution $Q$ provides another way to allocate weights of different types. This setup makes it possible to construct at least two possible null-model-type weighted networks:

(i.) the first is a network that has the same topology and weight distribution but, with weights allocated at random (i.e. ignoring degree-weight correlations) as prescribed by the random variable $W$ and its distribution $Q$, and

(ii.) the second is simply a weighted network where all link-weights are equal to the average weight computed as

$$\langle w \rangle_{dd} = \frac{\sum_{i=k_{min}}^{k_{max}} NP(i)i\frac{iP(i)}{\langle k \rangle}w_{ii} + 2\sum_{i=k_{min}}^{k_{max}-1}\sum_{j=i+1}^{k_{max}} NP(i)i\frac{jP(j)}{\langle k \rangle}w_{ij}}{\langle k \rangle N},$$

where $NP(i)i\frac{jP(j)}{\langle k \rangle} = \frac{ijNP(i)P(j)}{\langle k \rangle}$ stands for the actual expected number of links between nodes of degree $i$ and $j$, and $\langle k \rangle = \sum kP(k)$ is the average nodal degree.

These two null models will be used as baseline models for comparison when looking to determine the effect of degree-dependent weights on epidemic dynamics and other important indicators, such as $R_0$ and final epidemic size.

*2.1.3. Epidemic model and simulation*

In this paper, the simple *SIR* (susceptible-infective-recovered) epidemic model is considered. Disease transmission is specified in terms of infection and recovery events. The rate of transmission over an edge of weight 1 is denoted by $\tau$ and this is adjusted by the edge weight by assuming that transmission is directly proportional to it, i.e. rate of transmission across an edge of weight $w$ is $\tau w$. Infected individuals recover independently of each other at rate $\gamma$. The simulation is implemented using the Gillespie algorithm [2] with exponentially distributed (rate given by the total rate of change in the system) inter-event times,



https://doi.org/10.1051/mmnp/20149204 Published online by Cambridge University Press

with the single event to be implemented at each step being chosen at random and proportionally to its rate. All simulations start with a few infected nodes chosen at random with the remaining nodes being susceptible.

## 2.2. Approximate ODE models

Markovian processes on networks, being disease, rumour, information, innovation transmission or firing neurones result in an exact mathematical description in terms of Kolmogorov/master equations. Their high dimensionality, even for small networks, renders them difficult to use and often these can only be used to ascertain results of a theoretical nature but may offer less insight for specific applications. Notably, for highly symmetric or regular networks, the exact equations can be used directly and this is an area that has been well exploited and has been used to provide and illustrate linkages between stochastic and approximate ODE models. However, for more general networks, the drawback of the exact model remains. This has led to the development of a number of approaches and models that do an excellent job in approximating results from explicit simulations on networks which correspond to what would be regarded as the exact model. Examples include: (a) pairwise models [1, 11, 14, 18], (b) edge-based compartmental models and in general approaches that require the use of probability generating functions [6], (c) effective degree models [9,24], and other variations or combinations based around these. In this paper, we will concentrate on pairwise and edge-based compartmental models and will assess their flexibility and performance in accounting and approximating epidemic dynamics unfolding on two main classes of weighted networks.

### *2.2.1. Pairwise models*

The model extension that we propose is partly covered in Rattana *et al.* [20]. However, here we extend this from homogenous to heterogeneous networks with random weights as well as to the case where edge weights and node degree are not independent. Before writing down the two models, we refresh the notation and counting procedures. In line with the notation used for pairwise models, the number of singles remains unchanged, with $[A_k]$ denoting the number of nodes across the whole network which have degree $k$ and are in state $A$. Pairs of type $A_k - B_{k'}$, $[A_k B_{k'}]$, are now further divided depending on edge weights, i.e. $[A_k B_{k'}]_i$ represents the number of links of type $A_k - B_{k'}$ with the edge having weight $w_i$, where as before $i = 1, 2, \ldots, M$ and $A, B \in \{S, I, R\}$. Edges are doubly counted (e.g. in both directions) and thus the following relations hold: $[A_k B_{k'}]_m = [B_{k'} A_k]_m$ and $[A_k A_k]_m$ is equal to twice the number of uniquely counted links of weight $w_m$ with nodes at both ends in state $A$ and having degree $k$. From this extension it follows that $\sum_{i=1}^{M} [A_k B_{k'}]_i = [A_k B_{k'}]$. The same convention holds at the level of triples where $[A_k B_{k'} C_q]_{mn}$ stands for the expected number of triples where a node in state $B$ and of degree $k'$ connects a node in state $A$ and of degree $k$ and a node in state $C$ and of degree $q$ via links of weight $w_m$ and $w_n$, respectively. The weight of the edge impacts on the rate of transmission across that edge, and this is achieved by using a link-specific transmission rate equal to $\tau w_i$, where $i = 1, 2, \ldots, M$. In line with the above, we construct two pairwise models, one for randomly distributed weights across edges and one for the case where edge weights and node degrees are correlated.



https://doi.org/10.1051/mmnp/20149204 Published online by Cambridge University Press

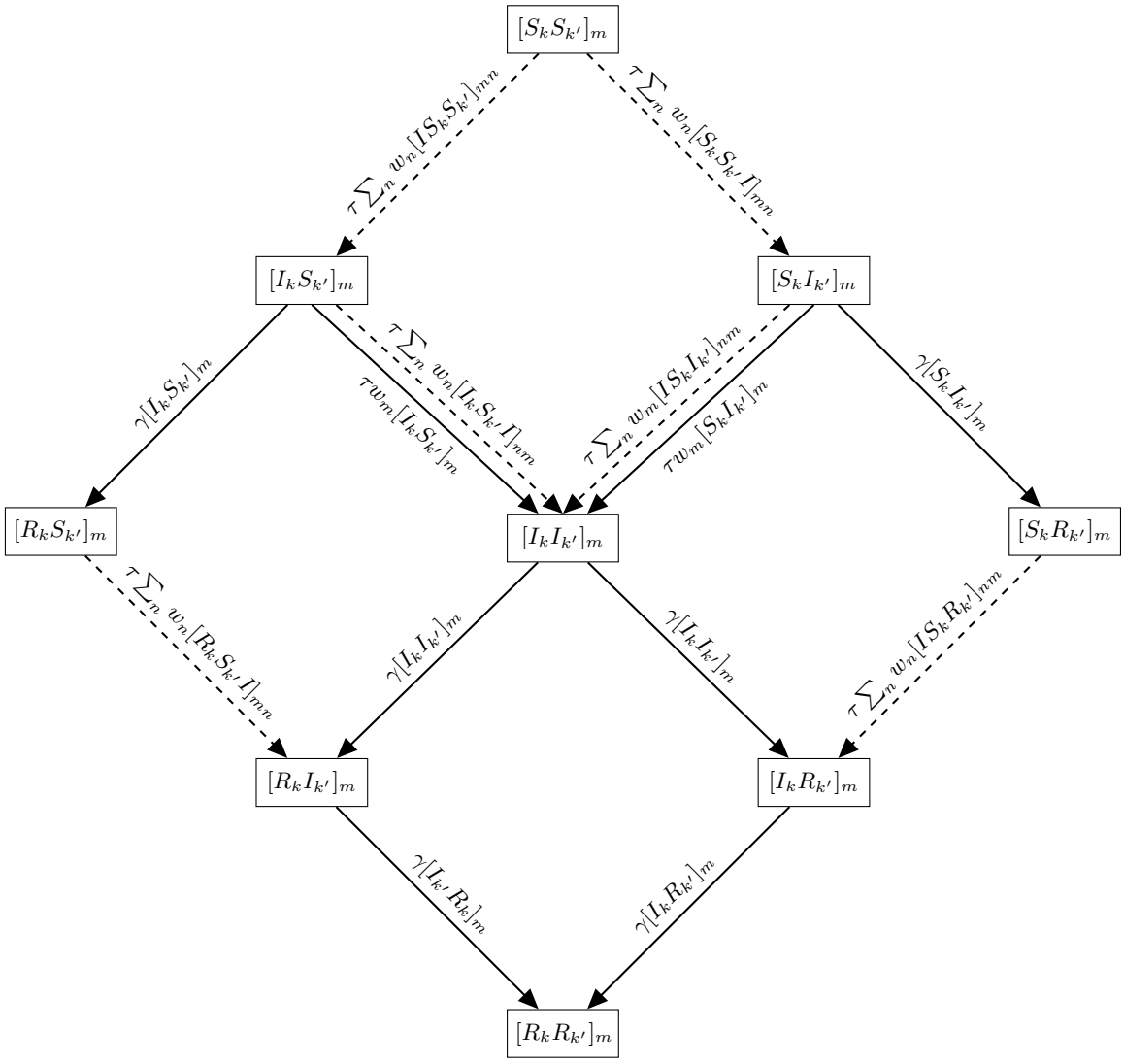



FIGURE 1. Flow diagram showing the evolution of pairs in the random weight case. The only pairs which have the potential to *eventually* transmit are the $[SS]$, $[SI]$ and $[IS]$ pairs, and hence, these need to be tracked. Solid and dashed arrows denote transmission within and from outside the pairs, respectively. We are able to find a closed system of equations which does not require calculating the other terms.

**Evolution equations for $SIR$ dynamics on heterogenous networks with random weights**

$$
\begin{aligned}
[\dot{S_k}] &= -\tau \textstyle\sum_{n=1}^{M} w_n [S_k I]_n, \\
[\dot{I}] &= \tau \textstyle\sum_k \sum_{n=1}^{M} w_n [S_k I]_n - \gamma [I], \\
[S_k \dot{S}_{k'}]_m &= -\tau \textstyle\sum_{n=1}^{M} w_n \left( [S_k S_{k'} I]_{mn} + [S_{k'} S_k I]_{mn} \right), \\
[\dot{S_k I}]_m &= \tau \left( \textstyle\sum_{k'} \sum_{n=1}^{M} w_n [S_k S_{k'} I]_{mn} - \sum_{n=1}^{M} w_n [I S_k I]_{nm} - w_m [S_k I]_m \right) - \gamma [S_k I]_m,
\end{aligned}
\tag{2.1}
$$



https://doi.org/10.1051/mmnp/20149204 Published online by Cambridge University Press

where $k, k' \in \{k_{min}, k_{min}+1, \ldots, k_{max}\}$ and $m = 1, 2, 3, ..., M$. Here, $k_{min}$ and $k_{max}$ stands for the smallest and largest nodal degree in the network. We further note that the system above stems from a reduction applied to a fuller version, see flow diagram in Fig. 1, where evolution equations for all $[I_k]$ classes are given (i.e. $[\dot{I}_k] = \tau \sum_{l=k_{min}}^{k_{max}} \sum_{n=1}^{M} w_n [S_k I_l]_n - \gamma[I_k]$). Summing this for $k = k_{min}, k_{min}+1, \ldots, k_{max}$ gives the evolution equations for $[I]$, as shown above. A similar notational procedure has been applied at the level of triples where in general $[A_k B_{k'} I]_{mn} = \sum_{q=k_{min}}^{k_{max}} [A_k B_{k'} I_q]_{mn}$.

The above system of Eq. (2.1) is not closed. Singles depend on pairs, and pairs depend on triples. Thus equations for triples are needed. This dependency on higher-order moments can be broken via approximating triples in terms of singles and pairs [18]. The agreement of the results from the closed system with simulation depends on how well the closure captures essential features of network structure and the edge weight distribution. Following Eames [14], the following closure is applied,

$$[A_m B_n I] = \frac{n-1}{n} \frac{[A_m B_n][B_n I]}{[B_n]} \text{ or } [A_m B_n C_p] = \frac{n-1}{n} \frac{[A_m B_n][B_n C_p]}{[B_n]}. \tag{2.2}$$

It is worth noting that the equations only rely on triples for which the central individual is susceptible. Thus individuals at the "ends" of a triple cannot affect one another's status through the central node until after they no longer affect the equations at the pair level.

**Evolution equations for $SIR$ dynamics on networks with degree-dependent weights**

The focus now shifts to the case where we wish to incorporate some general correlation between edge weights and nodal degree. This is done by assuming that transmission between a susceptible node of degree $k$ and an infected node of degree $q$ happens at rate $\tau w_{kq}$, where $w_{kq} = w(k, q)$ can accommodate various dependencies of edge weight on nodal degree. The pairwise equations follow in the same way as before and are given by

$$\begin{aligned}
[\dot{S}_k] &= -\tau \textstyle\sum_q w_{kq} [S_k I_q], \\
[\dot{I}_k] &= \tau \textstyle\sum_q w_{kq} [S_k I_q] - \gamma [I_k], \\
[\dot{S_k S_{k'}}] &= -\tau \textstyle\sum_q (w_{k'q} [S_k S_{k'} I_q] + w_{kq} [S_{k'} S_k I_q]), \\
[\dot{S_k I_{k'}}] &= \tau \textstyle\sum_q (w_{k'q} [S_k S_{k'} I_q] - w_{kq} [I_{k'} S_k I_q]) - \tau w_{kk'} [S_k I_{k'}] - \gamma [S_k I_{k'}],
\end{aligned} \tag{2.3}$$

where as before $k, k', q \in \{k_{min}, k_{min}+1, \ldots, k_{max}\}$ and with $w_{xy}$ yet unspecified. A corresponding flow diagram is given in Fig. 2. This system is closed in the same way as before using Eq. (2.2).

*2.2.2. Edge-based compartmental models for weighted networks*

We follow the derivation of Edge-based compartmental models (EBCM) of [4, 6, 7]. We assume that the population is connected according to the configuration model. We assume that the population-scale measures of infection (number infected, etc) are behaving deterministically. A consequence of this assumption is that if we choose a random individual $u$, the random event of whether $u$ is or is not infected cannot have any impact on the population scale. So if we alter a single individual $u$ so that $u$ can become infected but cannot transmit to its partners, this can have no population-scale impact.

We define a test individual as follows: $u$ is a test individual if $u$ is randomly selected from the population and prevented from transmitting to its neighbours. Because the dynamics are deterministic and $u$ is selected randomly, the probability $u$ is in a given state equals the proportion of the population in that state. So to calculate the proportion infected, we can simply calculate the probability $u$ is infected. This depends on the probabilities that the partners of $u$ are infected. Because we have prevented $u$ from causing any infections, the status of each partner of $u$ is independent of any other partner, which will simplify our calculations without altering the time of first infection of $u$. This is closely related to the



https://doi.org/10.1051/mmnp/20149204 Published online by Cambridge University Press

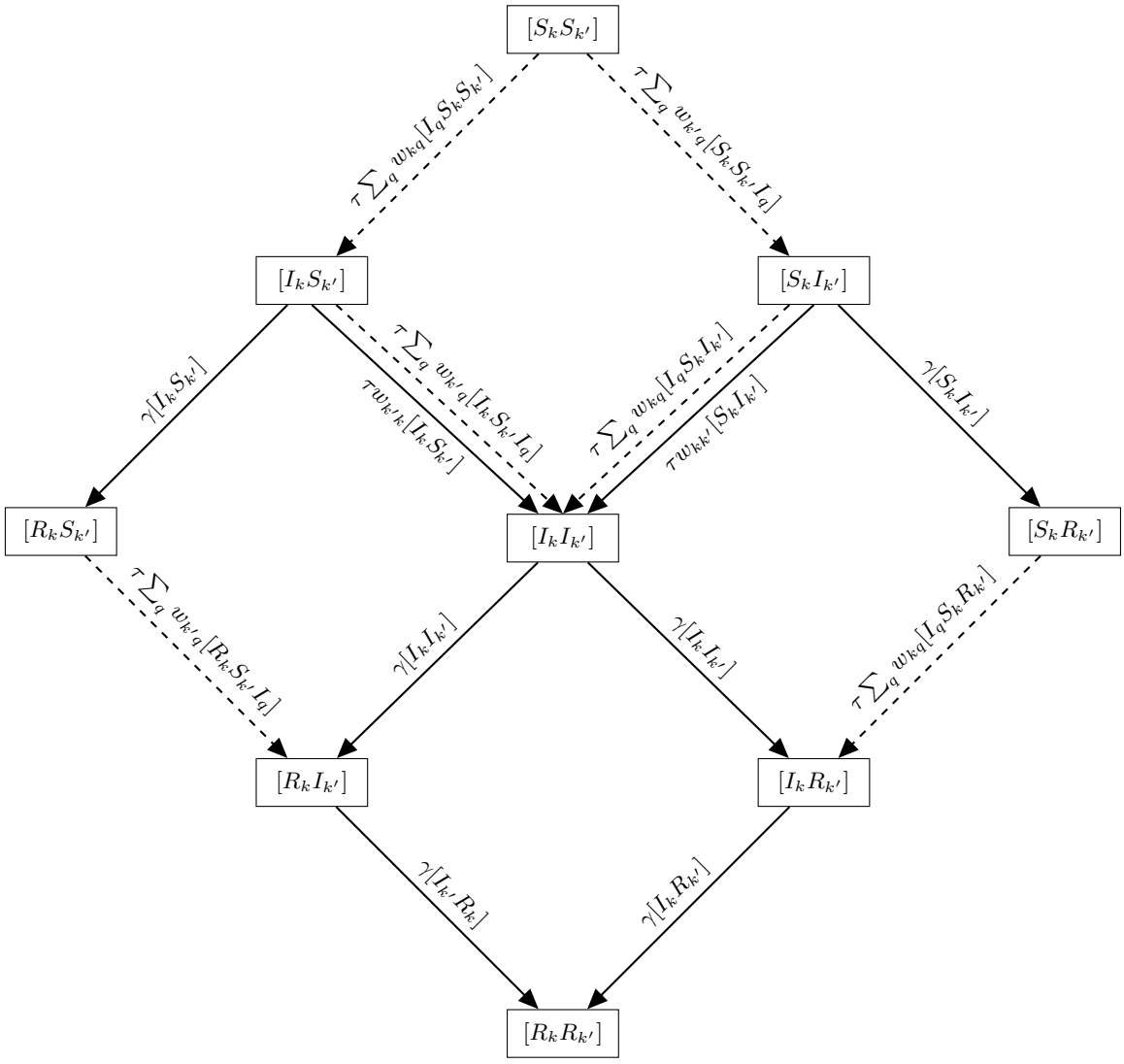



FIGURE 2. Flow diagram showing the evolution of pairs in the degree-dependent weight case. The only pairs which have the potential to *eventually* transmit are the $[SS]$, $[SI]$ and $[IS]$ pairs, and hence, these need to be tracked. Solid and dashed arrows denote transmission within and from outside the pairs, respectively. Again we are able to find a closed system of equations which only requires the $[SS]$, $[SI]$, and $[IS]$ terms.

observation for the pairwise equations that the triples only appear in the pair equations if the central individual is still susceptible.

**EBCM Evolution equations for $SIR$ dynamics on heterogeneous networks with random weights**

As before, let us assume that there is a weight distribution $Q(w)$ assigned to the edges. We assume that the transmission rate for an edge with a given $w$ is simply $\tau w$ for some parameter $\tau$. We further assume that; (a) infected individuals recover at rate $\gamma$, which is independent of how they were infected and that (b) at the initial time $t = t_0$, the probability an individual of degree $k$ is susceptible is $S(k, t_0)$.



https://doi.org/10.1051/mmnp/20149204 Published online by Cambridge University Press

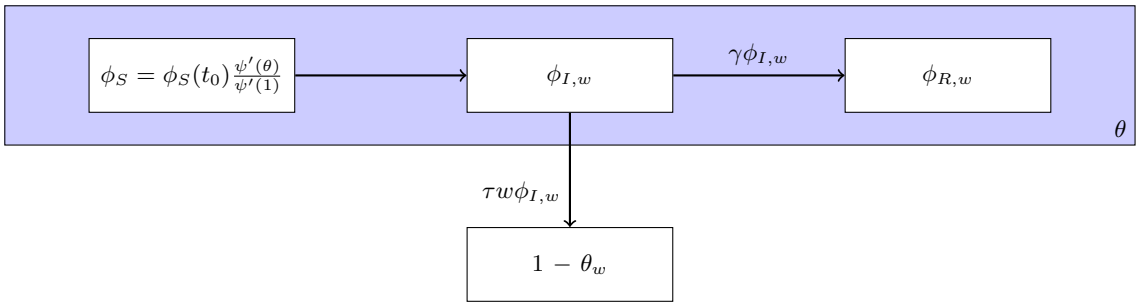



FIGURE 3. Flow diagram for EBCM model of random weight case. The large, shaded box contains all compartments, where transmission has not yet occurred.

Let us now consider a test individual $u$, and let $v$ be a random neighbour of $u$. Let $\theta$ be the probability that $v$ has not transmitted to $u$ given that at time $t_0$ $v$ had not yet transmitted to $u$. Then trivially, $\theta = \sum_w Q(w)\theta_w$ where $\theta_w$ is the probability a neighbour along a weight $w$ edge has not transmitted to $u$ given that it had not yet transmitted at time $t_0$. Note that $\theta(t_0) = 1$. These probabilities are not affected by the degree of $u$, so the probability $u$ is susceptible is

$$S(t) = \sum_k P(k)S(k,t_0)\theta^k = \psi(\theta).$$

Once we know $S(t)$, we can find the probability that $u$ is infected or recovered simply by noting that $\dot{R} = \gamma I$ and $I = 1 - S - R$.

To complete the system, all the $\theta_w$ need to specified. Assuming that the edge connecting $v$ to $u$ has weight $w$, we define $\phi_{S,w}$ to be the probability that $v$ is still susceptible. We define $\phi_{I,w}$ to be the probability $v$ is infected but has not transmitted to $u$. We define $\phi_{R,w}$ to be the probability $v$ has recovered and did not transmit to $u$. Then $\theta_w = \phi_{S,w} + \phi_{I,w} + \phi_{R,w}$ and $1 - \theta_w$ is the probability transmission has occurred (given that it had not occurred prior to $t_0$). Note however, that $\phi_{S,w}$ is independent of $w$ because the weight of the edge from $u$ to $v$ does not influence the probability $v$ has become infected. So we can treat $\phi_{S,w}$ as simply $\phi_S$.

To find $\phi_S(t)$, we assume its initial value $\phi_S(t_0)$ is known. We need to find the probability that $v$ has degree $k$ given that it was chosen as a neighbour of $u$ and was susceptible at time $t_0$. To do this, we count all edges belonging to susceptible nodes of degree $k$ at time $t_0$ and divide by the number of all edges belonging to susceptible nodes at time $t_0$. This yields $kP(k)S(k,t_0)N/\sum_{k'} k'P(k')S(k',t_0)N = kP(k)S(k,t_0)/\psi'(1)$. The probability that $v$ is still susceptible if it started susceptible and has degree $k$ is $\theta^{k-1}$. So $\phi_S(t) = \phi_S(t_0)\psi'(\theta)/\psi'(1)$. Note that this is independent of $w$.

We can find $\phi_{R,w}(t)$ in terms of $\theta_w$. We assume that its initial value $\phi_{R,w}(t_0)$ is known. By definition, $\theta_w(t_0) = 1$. An infected neighbor along a weight-$w$ edge transmits at rate $\tau w$ and recovers at rate $\gamma$. Thus it moves from being counted towards $\phi_{I,w}$ to being counted towards $\phi_{R,w}$ at rate $\gamma$ and to being counted towards $1 - \theta_w$ at rate $\tau w$. Thus the rate of increase of $\phi_{R,w}$ is $\gamma/\tau w$ times the rate of increase of $1 - \theta_w$. Using this argument, we conclude that

$$\phi_{R,w} = \frac{\gamma}{\tau w}(1 - \theta_w) + \phi_{R,w}(t_0).$$

The arguments above are summarised in Fig. 3.

Then, since $\phi_S + \phi_{I,w} + \phi_{R,w} = \theta_w$ and we know $\phi_S$ and $\phi_{R,w}$, we can compute $\phi_{I,w}$. Summarising the findings above leads to

$$\dot{\theta}_w = -\tau w\phi_{I,w}$$



https://doi.org/10.1051/mmnp/20149204 Published online by Cambridge University Press

$$= -\tau w \left( \theta_w - \phi_S(0) \frac{\psi'(\theta)}{\psi'(1)} - \frac{\gamma(1-\theta_w)}{\tau w} - \phi_{R,w}(0) \right),$$

So we end up with the system

$$\dot{\theta}_w = -\tau w \theta_w + \tau w \phi_S(0) \frac{\psi'(\theta)}{\psi'(1)} + \gamma(1-\theta_w) + \tau w \phi_{R,w}(t_0), \tag{2.4}$$

$$\theta = \sum_w Q(w) \theta_w, \tag{2.5}$$

where as for the pairwise model $w \in \{w_1, w_2, \ldots, w_M\}$. The initial conditions on $\phi_{S,w}(t_0)$ and $\phi_{R,w}(t_0)$ depend on how the epidemic is initialized. We have $\theta_w(t_0) = 1$. Noting that in $\psi'(\theta)$ it is $\theta$, not $\theta_w$, and combining the above with

$$S = \psi(\theta), \qquad I = 1 - S - R, \qquad \dot{R} = \gamma I,$$

completes the system.

In general starting by randomly selecting a proportion $\rho$ of individuals yields $S(k, t_0) = \phi_S(t_0) = 1 - \rho$ and $\phi_{R,w}(t_0) = R(t_0) = 0$. If instead the diseases starts with a very small number and set $t_0$ when enough infections are present to be deterministic, then the initial conditions are different, and depend on the state of the population at this initial time [4]. In particular $S(k, t_0)$ may depend on $k$ and not match exactly with $\phi_S(t_0)$.

**EBCM evolution equations for $SIR$ dynamics on networks with degree-dependent weights**
The focus now shifts to the case when across each edge there is a weight $w_{kk'} = w(k, k')$ which depends on the degrees $k$ and $k'$ of the neighbouring nodes. Transmission happens at rate $\tau w_{kk'}$. We define $\theta_k$ to be the probability a neighbour of a degree $k$ test node has not transmitted to it (given that it had not at time $t_0$). Due to this being $k$ dependent, the expression for $\psi(\theta)$ will be more complicated compared to the random weights case. Instead, the probability the test node is susceptible is

$$S(t) = \sum_k P(k) S(k, t_0) \theta_k^k = \psi(\theta_{k_{min}}, \theta_{k_{min}+1}, \ldots, \theta_{k_{max}}).$$

Assume the neighbor $v$ has degree $k'$. We define $\theta_{k,k'}$ to be the probability that $v$ has not transmitted given that it has degree $k'$, $u$ has degree $k$, and $v$ had not transmitted to $u$ by time $t_0$. Then $v$ is in the same states as before with probabilities $\phi_{S,k,k'}(t)$, $\phi_{I,k,k'}(t)$, and $\phi_{R,k,k'}(t)$. We find $\phi_{S,k,k'}(t) = \phi_{S,k,k'}(t_0) \theta_{k'}^{k'-1}$. We find that $\phi_{R,k,k'} = \gamma(1 - \theta_{k,k'})/\tau w_{kk'} + \phi_{R,k,k'}(t_0)$. The picture underlying this process of thought is given in Fig. 4.

The final equations are

$$\dot{\theta}_{k,k'} = -\tau w_{kk'} \theta_{k,k'} + \tau w_{kk'} \phi_{S,k,k'}(t_0) \theta_{k'}^{k'-1} + \gamma(1 - \theta_{k,k'}) + \tau w_{kk'} \phi_{R,k,k'}(t_0), \tag{2.6}$$

$$\theta_k = \sum_{k'} P_n(k, k') \theta_{k,k'}, \tag{2.7}$$

$$\dot{R} = \gamma I, \qquad I = 1 - S - R, \qquad S = \sum_k P(k) S(k, t_0) \theta_k^k, \tag{2.8}$$

where $P_n(k, k')$ is the probability the neighbour of $u$ has degree $k'$ given that it hadn't transmitted to $u$ by time $t_0$.

As before if we start by randomly selecting a proportion $\rho$ of individuals at time $t_0$, we have $S(k, t_0) = \phi_{S,k,k'}(t_0) = 1 - \rho$, and $\phi_{R,k,k'}(t_0) = R(t_0) = 0$. In this case we get $P_n(k, k') = k' P(k') / \sum_{k''} k'' P(k'')$. Hence, if the initial infected proportion is a randomly chosen proportion $\rho$, then the initial conditions are:

$$R(t_0) = 0,$$



https://doi.org/10.1051/mmnp/20149204 Published online by Cambridge University Press

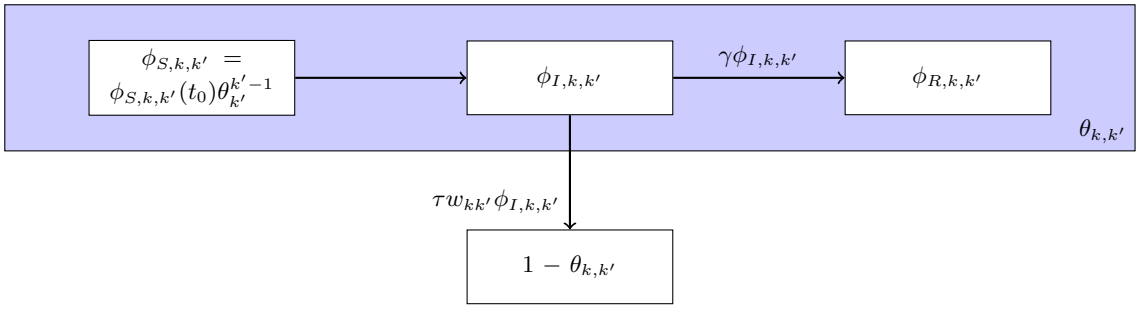



FIGURE 4. Flow diagram for the EBCM model with weights dependent on degree. The large, shaded box contains all compartments, where transmission has not yet occurred.

$$\begin{aligned}\phi_{R,k,k'}(t_0) &= 0,\\ S(k,t_0) &= 1-\rho,\\ \phi_{S,k,k'}(t_0) &= 1-\rho,\\ \theta_{k,k'}(t_0) &= 1,\end{aligned}$$

and

$$P_n(k,k') = \frac{k'P(k')}{\langle k\rangle}.$$

If the disease has been spreading for some time, the considerations above will not hold. In many cases, $P_n(k,k')$ can be calculated rather than taken as an 'initial condition'. If the infection has been spreading for some time before $t_0$, then the probability a neighbour has transmitted to $u$ before $t_0$ depends on the degree of the neighbour. Since we define $\theta$ to be conditional on transmission to $u$ never happening prior to $t_0$, this needs to be corrected for, and thus $P_n(k,k')$ will be different.

## 3. Results

In this section we present analytical and numerical results from network simulations, pairwise and edge-based representations of $SIR$ dynamics. To compute the early growth rate and final epidemic size, we first write out the edge-based system for the special case of a heterogeneous network with low (degree $l$ with probability $P(l)$) and high (degree $h$ with probability $P(h)$) degree. This automatically induces three weights $w_1 = w_{ll}$, $w_2 = w_{lh} = w_{hl}$ and $w_3 = w_{hh}$. Moreover, for the degree-dependent weighted network, the distribution of weights is given by: $q_1 = q_{ll} = \frac{l^2P^2(l)}{\langle k\rangle^2}$, $q_2 = q_{lh} = q_{hl} = \frac{2lhP(l)P(h)}{\langle k\rangle^2}$ and $q_3 = q_{hh} = \frac{h^2P^2(h)}{\langle k\rangle^2}$, where $\langle k\rangle = lP(l) + hP(h)$ is the average nodal degree, and $q_2$ stands for the proportion of uniquely counted links between $l$ and $h$ nodes.

### 3.1. Epidemic threshold and final epidemic size

While pairwise models can be used to compute $R_0$ [18] and early growth rate [20], this is only practical for special cases where the number of equations remains relatively low. Such calculations are possible for homogenous unweighted networks [18] and even for homogenous networks with two different edge weight types [12, 20]. In general and as we show, the edge-based compartmental models are more amenable to such analysis due to their smaller dimensionality, see Table 1.



https://doi.org/10.1051/mmnp/20149204 Published online by Cambridge University Press

TABLE 1. System complexity in terms of the number of differential equations needed to fully describe the epidemic dynamics. As before, $M$ is the number of different weight types and $K$ is the number of different nodal degrees, e.g. $K = k_{max} - k_{min} + 1$ provided that nodes of any degree between minimum and maximum degree exist.

| Type of weighted network | Pairwise model | Edge-based model |
|---|---|---|
| randomly distributed weights | full system: $2K + \frac{K(K+1)}{2}M + K^2M$<br>reduced-system : $K + 1 + \frac{K(K+1)}{2}M + KM$ | $M + 1$ |
| degree-dependent weights | $2K + \frac{K(K+1)}{2} + K^2$ | $K^2 + 1$ |

*3.1.1. Random edge weight distribution for heterogeneous networks*

The three weights system leads to working with $\theta_{w_1}, \theta_{w_2}$ and $\theta_{w_3}$, where $Q(w_1) = q_1, Q(w_2) = q_2$ and $Q(w_3) = 1 - q_1 - q_2 = q_3$. Based on Eq. (2.4), the evolution equations for these are,

$$\dot{\theta}_{w_1} = -\tau w_1 \theta_{w_1} + (1-\rho)\tau w_1 \frac{\psi'_{\theta_{w_1}}(\theta)}{\psi'_{\theta_{w_1}}(1)} + \gamma(1-\theta_{w_1}), \tag{3.1}$$

$$\dot{\theta}_{w_2} = -\tau w_2 \theta_{w_2} + (1-\rho)\tau w_2 \frac{\psi'_{\theta_{w_2}}(\theta)}{\psi'_{\theta_{w_2}}(1)} + \gamma(1-\theta_{w_2}), \tag{3.2}$$

$$\dot{\theta}_{w_3} = -\tau w_3 \theta_{w_3} + (1-\rho)\tau w_3 \frac{\psi'_{\theta_{w_3}}(\theta)}{\psi'_{\theta_{w_3}}(1)} + \gamma(1-\theta_{w_3}). \tag{3.3}$$

For a heterogenous network with $N$ nodes where a node has degree $l$ (e.g. low degree) with probability $P(l)$ or degree $h$ (e.g. high degree) with probability $P(h) = 1 - P(l)$, the proportion of susceptibles at time $t$ (based on Eq. (2.5)) is given by

$$S(t) = (1-\rho)(P(l)\theta^l + P(h)\theta^h) = \psi(\theta),$$

where $\theta = q_1\theta_{w_1} + q_2\theta_{w_2} + q_3\theta_{w_3}$.

**Early growth rate**

To compute the early growth rate, the assumption of an infinitesimally small initial infection must hold. Hence, to satisfy this requirement, we modify Eqs. (3.1-3.3) by taking $(1-\rho) \to 1$. This gives

$$\begin{aligned}
\dot{\theta}_{w_1} &= -\tau w_1 \theta_{w_1} + \tau w_1 \left[P_e(l)\theta^{l-1} + P_e(h)\theta^{h-1}\right] + \gamma(1-\theta_{w_1}),\\
\dot{\theta}_{w_2} &= -\tau w_2 \theta_{w_2} + \tau w_2 \left[P_e(l)\theta^{l-1} + P_e(h)\theta^{h-1}\right] + \gamma(1-\theta_{w_2}),\\
\dot{\theta}_{w_3} &= -\tau w_3 \theta_{w_3} + \tau w_3 \left[P_e(l)\theta^{l-1} + P_e(h)\theta^{h-1}\right] + \gamma(1-\theta_{w_3}),
\end{aligned}$$

where $P_e(l) = lP(l)/\langle k\rangle$, $P_e(h) = hP(h)/\langle k\rangle$ and $\langle k\rangle = lP(l) + hP(h)$. Here, $P_e(k)$ represents the probability of finding a node of degree $k$ when picking an edge at random and considering either of the nodes at its ends. We set $\theta_{w_1} = 1+\varepsilon_1, \theta_{w_2} = 1+\varepsilon_2$ and $\theta_{w_3} = 1+\varepsilon_3$. We linearise about the equilibrium and have the matrix equation

$$\begin{pmatrix} \dot{\varepsilon_1} \\ \dot{\varepsilon_2} \\ \dot{\varepsilon_3} \end{pmatrix} = \begin{pmatrix} -\tau w_1 + \tau w_1 q_1 \zeta - \gamma & \tau w_1 q_2 \zeta & \tau w_1 q_3 \zeta \\ \tau w_2 q_1 \zeta & -\tau w_2 + \tau w_2 q_2 \zeta - \gamma & \tau w_2 q_3 \zeta \\ \tau w_3 q_1 \zeta & \tau w_3 q_2 \zeta & -\tau w_3 + \tau w_3 q_3 \zeta - \gamma \end{pmatrix} \begin{pmatrix} \varepsilon_1 \\ \varepsilon_2 \\ \varepsilon_3 \end{pmatrix},$$



https://doi.org/10.1051/mmnp/20149204 Published online by Cambridge University Press

where

$$\zeta = (l-1)P_e(l) + (h-1)P_e(h).$$

Thus, the eigenvalues are the solutions of a 3rd order equation given by $\lambda^3 + a_1\lambda^2 + a_2\lambda + a_3 = 0$, where

$$\begin{aligned} a_1 &= u_1 + u_2 + u_3 - v_1 - v_2 - v_3, \\ a_2 &= u_1u_2 + u_1u_3 + u_2u_3 - u_1(v_2+v_3) - u_2(v_1+v_3) - u_3(v_1+v_2), \\ a_3 &= u_1u_2u_3 - u_1u_2v_3 - u_1u_3v_2 - u_2u_3v_1, \end{aligned}$$

where, $u_i$-s and $v_i$-s are given by

$$u_i = \tau w_i + \gamma\,, \quad v_i = \tau w_i q_i \zeta \quad \text{for} \quad i = 1,2,3.$$

By considering the case of $\lambda = 0$, the critical point for change of stability, the third order equation yields $a_3 = 0$. This means that at the point at which the eigenvalue changes sign $a_3 = 0$, and this gives a relation between the system parameters which determines the threshold condition.

**The basic reproduction number - $R_0$**

The basic reproduction number $R_0$ can be computed in two different ways. First, by using an individual-level view and average across nodes of different degrees that have become infected from the very initial index case. By doing this, we average the expected number of infections in the second generation. This approach yields,

$$R_0^{rw} = (l-1)P_e(l)(q_1r_1 + q_2r_2 + q_3r_3) + (h-1)P_e(h)(q_1r_1 + q_2r_2 + q_3r_3),$$

where

$$r_i = \frac{\tau w_i}{\tau w_i + \gamma} \quad \text{for} \quad i = 1,2,3.$$

A more rigorous and widely applicable approach is to compute $R_0$ as the leading eigenvalue of the next generation matrix (NGM). In this case, we can consider the epidemic in terms of an embedded multi-type branching process [3, 10], where the $NGM = (m_{ij})_{i,j=1,2,\ldots,N_t}$ ($N_t$ - number of different types) consists of entries giving the expected number of offsprings of type $i$ produced by a single individual of type $i$. Once, the different types have been defined, then NGM can be constructed, and $R_0$ will be equivalent to the leading eigenvalue of the NGM. In this case, we have individuals of two different types (individuals of low and high degree) and the NGM is given by,

$$NGM = \begin{bmatrix} (l-1)P_e(l)(q_1r_1 + q_2r_2 + q_3r_3) & (h-1)P_e(l)(q_1r_1 + q_2r_2 + q_3r_3) \\ (l-1)P_e(h)(q_1r_1 + q_2r_2 + q_3r_3) & (h-1)P_e(h)(q_1r_1 + q_2r_2 + q_3r_3) \end{bmatrix},$$

where, for example $(h-1)P_e(l)(q_1r_1 + q_2r_2 + q_3r_3)$ stands for the expected number of individuals of low degree infected by a typical infected individual with high degree. Hence,

$$R_0^{rw} = \Big((l-1)P_e(l) + (h-1)P_e(h)\Big)(q_1r_1 + q_2r_2 + q_3r_3), \tag{3.4}$$

and this is identical to the previously computed value. A further consistency check of our calculations can be performed. Namely, the relation $R_0^{rw} = 1 \Leftrightarrow \lambda = 0$ should hold. Indeed, using condition $a_3 = 0$ leads to $R_0^{rw} = 1$.

**Final epidemic size**

To compute the final epidemic size, we need to return to the original equations that account for the initial conditions as given by Eqs. (3.1-3.3). By setting the derivatives to zero, it is possible to find asymptotic values of $\theta_{w_1}$, $\theta_{w_2}$ and $\theta_{w_3}$, i.e. $\theta_{w_1}(\infty)$, $\theta_{w_2}(\infty)$ and $\theta_{w_3}(\infty)$. Once these values are known the final



https://doi.org/10.1051/mmnp/20149204 Published online by Cambridge University Press

epidemic size is given by $R(\infty) = 1 - \psi(\theta_{w_1}(\infty), \theta_{w_2}(\infty), \theta_{w_3}(\infty))$, where $\theta_{w_1}(\infty), \theta_{w_2}(\infty)$ and $\theta_{w_3}(\infty)$ are the solutions of the following system,

$$\theta_{w_1}(\infty) = \frac{\gamma + (1-\rho)\tau w_1 \left[P_e(l)\left(\theta(\infty)\right)^{l-1} + P_e(h)\left(\theta(\infty)\right)^{h-1}\right]}{\tau w_1 + \gamma}, \tag{3.5}$$

$$\theta_{w_2}(\infty) = \frac{\gamma + (1-\rho)\tau w_2 \left[P_e(l)\left(\theta(\infty)\right)^{l-1} + P_e(h)\left(\theta(\infty)\right)^{h-1}\right]}{\tau w_2 + \gamma}, \tag{3.6}$$

$$\theta_{w_3}(\infty) = \frac{\gamma + (1-\rho)\tau w_3 \left[P_e(l)\left(\theta(\infty)\right)^{l-1} + P_e(h)\left(\theta(\infty)\right)^{h-1}\right]}{\tau w_3 + \gamma}, \tag{3.7}$$

where $\theta(\infty) = q_1\theta_{w_1}(\infty) + q_2\theta_{w_2}(\infty) + q_3\theta_{w_3}(\infty)$. By treating the above as a fixed point problem, it can be shown that a numerical recursion will converge quickly to the true solution and we compare this simulation results in the numerical analysis part.

*3.1.2. Degree-dependent weights*

For the same simplified scenario with a network with bimodal degree distribution and weights that correlate with node-degree, Eqs. (2.6-2.8) yield

$$\dot{\theta}_{ll} = -\tau w_{ll}\theta_{ll} + (1-\rho)\tau w_{ll}\theta_l^{l-1} + \gamma(1-\theta_{ll}), \tag{3.8}$$

$$\dot{\theta}_{lh} = -\tau w_{lh}\theta_{lh} + (1-\rho)\tau w_{lh}\theta_h^{h-1} + \gamma(1-\theta_{lh}), \tag{3.9}$$

$$\dot{\theta}_{hl} = -\tau w_{hl}\theta_{hl} + (1-\rho)\tau w_{hl}\theta_l^{l-1} + \gamma(1-\theta_{hl}), \tag{3.10}$$

$$\dot{\theta}_{hh} = -\tau w_{hh}\theta_{hh} + (1-\rho)\tau w_{hh}\theta_h^{h-1} + \gamma(1-\theta_{hh}). \tag{3.11}$$

According to the model derivation $\theta_l$ and $\theta_h$ can be found as

$$\theta_l = P_n(l,l)\theta_{ll} + P_n(l,h)\theta_{lh},$$
$$\theta_h = P_n(h,l)\theta_{hl} + P_n(h,h)\theta_{hh},$$

with $P_n(k,k') = k'P(k')/\langle k\rangle$. This complemented by

$$S(t) = (1-\rho)(P(l)\theta_l^l + P(h)\theta_h^h),$$

gives the full system.

**Early growth rate**

As before, we note that for the correct calculation of the early growth rate, Eqs. (3.8-3.11) must be used with $(1-\rho) \to 1$. By setting $\theta_{ll} = 1+\varepsilon_1$, $\theta_{lh} = 1+\varepsilon_2$, $\theta_{hl} = 1+\varepsilon_3$ and $\theta_{hh} = 1+\varepsilon_4$, and linearising around the disease-free steady state leads to the following Jacobian,

$$J = \begin{bmatrix} -\tau w_1 + v_1 - \gamma & \tau w_1(l-1)P_n(l,h) & 0 & 0 \\ 0 & -\tau w_2 - \gamma & \tau w_2(h-1)P_n(h,l) & \tau w_2(h-1)P_n(h,h) \\ \tau w_2(l-1)P_n(l,l) & \tau w_2(l-1)P_n(l,h) & -\tau w_2 - \gamma & 0 \\ 0 & 0 & \tau w_3(h-1)P_n(h,l) & -\tau w_3 + v_2 - \gamma \end{bmatrix},$$

where

$$v_1 = \tau w_1(l-1)P_n(l,l)\,, \qquad v_2 = \tau w_3(h-1)P_n(h,h).$$



https://doi.org/10.1051/mmnp/20149204 Published online by Cambridge University Press

The eigenvalues will be the solution of $\det(J - \lambda I) = 0$, where $I$ is the identity matrix. Thus, the eigenvalues are the solutions of a 4th order equation given by $\lambda^4 + a_1\lambda^3 + a_2\lambda^2 + a_3\lambda + a_4 = 0$, where

$$
\begin{aligned}
a_1 &= u_1(1-R_1) + 2u_2 + u_3(1-R_2),\\
a_2 &= 2u_2\Big(u_1(1-R_1) + u_3(1-R_2)\Big) + u_2^2 + u_1u_3(1-R_1)(1-R_2) - v_3,\\
a_3 &= 2u_1u_2u_3(1-R_1)(1-R_2) + u_2^2\left(u_1(1-R_1) + u_3(1-R_2)\right) - v_3\left(u_1 + u_3(1-R_2)\right) - v_2v_3,\\
a_4 &= u_1u_2^2u_3(1-R_1)(1-R_2) - u_1u_3v_3(1-R_2) - u_1v_2v_3,
\end{aligned}
$$

where

$$
R_1 = (l-1)P_n(l,l)r_1, \qquad R_2 = (h-1)P_n(h,h)r_3, \qquad v_3 = (\tau w_2)^2(l-1)P_n(h,l)(h-1)P_n(l,h),
$$

and where $u_i$-s are given by

$$
u_i = \tau w_i + \gamma \quad \text{for} \quad i = 1,2,3.
$$

By considering the case of $\lambda = 0$, the critical point for change of stability, the fourth order equation yields $a_4 = 0$. This means that at the point at which the eigenvalue changes sign $a_4 = 0$, and this gives a threshold condition. As expected, it can be shown that $a_4 = 0$ is equivalent to $R_0^{dd} = 1$ (below). This confirms that the calculations are consistent.

**The basic reproduction number -** $R_0$

In this case, we calculate $R_0$ only by using the next generation matrix approach, and $R_0$ is the leading eigenvalue of the next generation matrix. Before writing down the NGM we need to specify the choice of individual types, and then the entries of the $NGM = (m_{ij})_{i,j=1,2,\ldots,N_t}$. For this case, the types will be depend solely on the degree of the nodes, and thus, the NGM is given by,

$$
NGM = \begin{bmatrix} (l-1)P_e(l)r_1 & (h-1)P_e(l)r_2 \\ (l-1)P_e(h)r_2 & (h-1)P_e(h)r_3 \end{bmatrix}.
$$

For example, the expected number of low degree individuals produced by a single high degree individual $h$, is given by $(h-1)P_e(l)r_2$. The leading eigenvalue of the above matrix, and thus $R_0$ is given by

$$
R_0^{dd} = \frac{R_1 + R_2 + \sqrt{(R_1 - R_2)^2 + 4F}}{2},
$$

where

$$
R_1 = (l-1)P_e(l)r_1, \qquad R_2 = (h-1)P_e(h)r_3,
$$

and

$$
F = (l-1)P_e(l)(h-1)P_e(h)r_2^2.
$$

**Final epidemic size**

Using the same approach as before and taking into account the initial condition in terms of $\rho$, the final epidemic size is given by $R(\infty) = 1 - \psi(\theta_l(\infty), \theta_h(\infty))$ where $\theta_{ll}(\infty)$, $\theta_{lh}(\infty)$, $\theta_{hl}(\infty)$ and $\theta_{hh}(\infty)$ are the solutions of the following system,

$$
\theta_{ll}(\infty) = \frac{\gamma + (1-\rho)\tau w_{ll}\theta_l^{l-1}(\infty)}{\tau w_{ll} + \gamma}, \tag{3.12}
$$

$$
\theta_{lh}(\infty) = \frac{\gamma + (1-\rho)\tau w_{lh}\theta_h^{h-1}(\infty)}{\tau w_{lh} + \gamma}, \tag{3.13}
$$

$$
\theta_{hl}(\infty) = \frac{\gamma + (1-\rho)\tau w_{hl}\theta_l^{l-1}(\infty)}{\tau w_{hl} + \gamma}, \tag{3.14}
$$

$$
\theta_{hh}(\infty) = \frac{\gamma + (1-\rho)\tau w_{hh}\theta_h^{h-1}(\infty)}{\tau w_{hh} + \gamma}. \tag{3.15}
$$



https://doi.org/10.1051/mmnp/20149204 Published online by Cambridge University Press

*3.1.3. Comparison of $R_0$ and final epidemic size*

Based on the analytic and semi-analytic calculations above, we provide a few examples where $R_0$ and the final epidemic size (Fig. 5) are compared for networks with heterogenous degree and weight distributions. Namely, as indicated in section 2.1, we start from networks with degree-dependent weights and compare $R_0$ and final epidemic size corresponding to this against those from networks with the same topology and same weight distribution but with weights assigned at random, and weighted networks where all weights are equal to the average weight from the original network, $\langle w\rangle_{dd} = q_1w_1 + q_2w_2 + q_3w_3$. Fig. 5 (top panel) shows clearly that $R_0$ is maximised when all weights are equal, and that networks with randomly distributed weights allow for a larger $R_0$ value compared to the case of networks where degrees and weights are inversely correlated. This observation can be made rigorous. We start by noting that $R_0$ for the case of equal weights, based on Eq. (3.4), is given by,

$$R_0^{av} = ((l-1)P_e(l) + (h-1)P_e(h))\frac{\tau\langle w\rangle_{dd}}{\tau\langle w\rangle_{dd}+\gamma}. \tag{3.16}$$

Similarly, based on Eq. (3.4), the basic reproduction ratio is given by

$$R_0^{rw} = ((l-1)P_e(l) + (h-1)P_e(h))\left(q_1\frac{\tau w_1}{\tau w_1+\gamma} + q_2\frac{\tau w_2}{\tau w_2+\gamma} + q_3\frac{\tau w_3}{\tau w_3+\gamma}\right).$$

First, we want to show that $R_0^{rw} \le R_0^{av}$. Noting that $\varphi(w) = \frac{\tau w}{\tau w+\gamma}$ is a concave function on $w \in [0,\infty)$, as $\varphi'' < 0$, then using Jensen's inequality under the condition $q_1 + q_2 + q_3 = 1$, yields

$$q_1\varphi(w_1) + q_2\varphi(w_2) + q_3\varphi(w_3) \le \varphi(q_1w_1 + q_2w_2 + q_3w_3),$$
$$q_1\frac{\tau w_1}{\tau w_1+\gamma} + q_2\frac{\tau w_2}{\tau w_2+\gamma} + q_3\frac{\tau w_3}{\tau w_3+\gamma} \le \frac{\tau(q_1w_1 + q_2w_2 + q_3w_3)}{\tau(q_1w_1 + q_2w_2 + q_3w_3)+\gamma}.$$

Hence, we can conclude that $R_0^{rw} \le R_0^{av}$, with equality when all weights are equal. Moreover, it is easy to see that when $w_1 = w_2 = w_3 = w$, we have

$$R_0^{rw} = R_0^{av} = ((l-1)P_e(l) + (h-1)P_e(h))\frac{\tau w}{\tau w+\gamma}.$$

In Appendix A, we also provide a rigorous proof for the observation that $R_0^{dd} \le R_0^{rw}$. Hence the following inequality holds

$$R_0^{dd} \le R_0^{rw} \le R_0^{av}. \tag{3.17}$$

We note that while the proof of $R_0^{rw} \le R_0^{av}$ does not rely on the negative correlation between degree and weight, the proof of the second inequality, $R_0^{dd} \le R_0^{rw}$, makes use of this information. The final epidemic size can be computed semi-analytically using the approach developed in the context of edge-based modelling. Namely, we use Eqs. (3.5 - 3.7) for the randomly-distributed and fixed weights case, and Eqs. (3.12 - 3.15) for the degree-dependent weighted network case. In both situations, we treat the equations as maps which we then numerically iterate to find their fixed points. The final epidemic size plots (see the bottom panel of Fig. 5) show that for the same $R_0$ value, the final epidemic size is largest on the original network with degree-dependent weights. This is a direct consequence of the relation between the $R_0$ values on the different networks, see Eq. (3.17). Namely, with all parameters being equal, $R_0$ is smallest on the original network. Hence, considering a fixed value of $R_0(= R_0^{const})$ across the different networks requires a larger value of $\tau$ on the original network compared to the randomly distributed and fixed weights cases. This higher value is required to compensate for the negative correlation between degree and weights, which means that $\tau$ has to be disproportionately large to compensate for the smallest possible weights between highly connected nodes. This increase in $\tau$ has an automatic knock on effect of also improving transmission between poorly connected nodes with an overall increase in final epidemic size. It is worth noting the complete reversion of order between the top and bottom panel of Fig. 5. The same



https://doi.org/10.1051/mmnp/20149204 Published online by Cambridge University Press

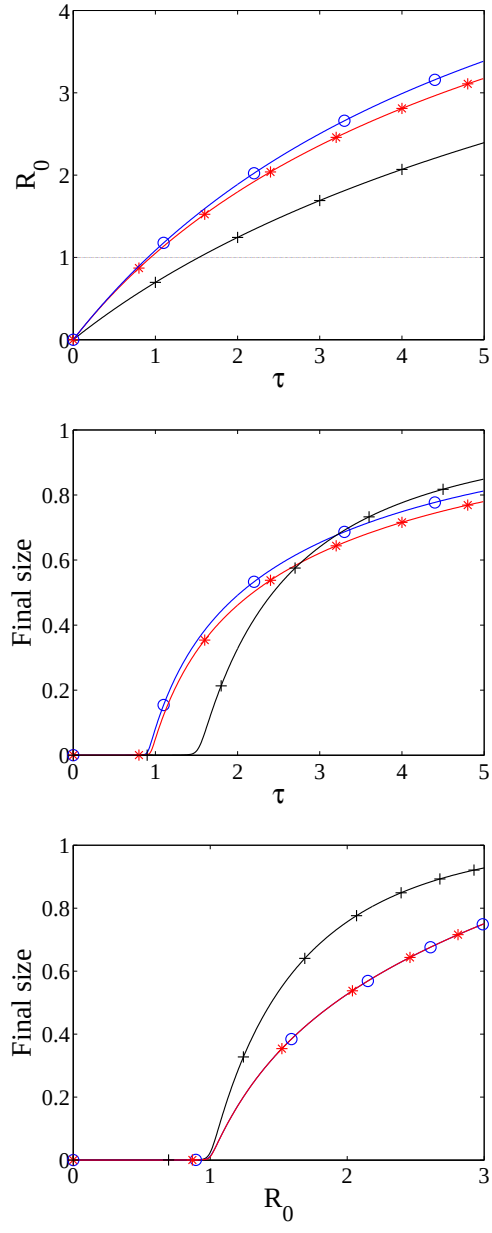



FIGURE 5. Basic reproductive ratio $R_0$ and final epidemic size for heterogeneous weighted networks. The parameters values are $\rho = 0.0001$, $P(l) = 0.8$, $P(h) = 1 - P(l)$, $l = 3$, $h = 13$ and $\gamma = 1$. Degree-dependent weighted networks (black line and $(+)$), networks with random weight distribution (red line and $(\star)$), and networks with all weights equal (blue line and $(\circ)$). All networks have the same average weight $\langle w \rangle_{dd} = q_1 w_{ll} + q_2 w_{lh} + q_3 w_{hh}$, where the weight function is $w_{ij} = 1/(i \times j)^{1/2}$.



https://doi.org/10.1051/mmnp/20149204 Published online by Cambridge University Press

figure shows that the random and uniform average weight cases lead to an identical functional relation between final epidemic size and $R_0$. In Appendix B, we provide a simple, formal proof for this observation.

**Final epidemic size comparisons**

To explore the potential of the various models to capture the final epidemic size, we compare outputs from the semi-analytic approach with long-time results from simulations and the long-time solution of the pairwise model. To stress test the robustness of the model, we use two additional weight functions, namely $w_{ij} = 1/(i+j)^{1/2}$ and $w_{ij} = 1/\ln(i+j)$. Numerical results presented in Fig. 6 exhibit excellent agreement across all models and for the three different weight functions. As opposed to Fig. 5, here we use a higher number of initially infected nodes ($I_0 = 50$ out of $N = 1000$) to avoid early stochastic extinction in simulations. The plots in Fig. 6 show a similar trend with that observed in Fig. 5 (see middle panel).

A notable feature is the changeover in the size of the final epidemic size from being larger on networks with randomly distributed weights (for smaller values of $\tau$) to the epidemic affecting a higher fraction of the population on networks with degree-dependent weights (for larger $\tau$ values). Intuitively this can be explained as follows. For degree-dependent weights, the transmissibility amongst, from or to highly connected nodes is penalised by small edge weights, with the smallest weights on high-to-high nodes connections. However, nodes that are less well connected can receive and transmit the infection more readily. We now discuss separately the cases of small and large $\tau$:

1. For small values of $\tau$, the random redistribution of weights will lead to links between, from or to highly connected nodes to be more likely to transmit, and this will lead to a larger final epidemic size. Transmission between poorly connected nodes will suffer but, infection involving highly connected nodes dominates for small values of $\tau$.
2. As the value of $\tau$ increases the effect of small weights is less significant (i.e. transmission rate is the product of weight and the value of $\tau$). Thus, disease spreads more readily across the whole network. However, redistributing links at random will improve an already appropriate transmission between highly-connected nodes (i.e. edge weights will always be greater or equal than for the degree-dependent weight case) but, at the expense of seeing smaller weights between less well connected nodes that are more abundant in the network.

The arguments above are confirmed by numerical simulations (not shown here), whereby the number of poorly connected, susceptible nodes at large times is greater in the case of random weights. All the effects above become less marked for the two additional weight functions. This is due to the two additional weight functions giving rise to higher edge weights, and thus a more efficient transmission with the epidemic affecting a large proportion of the network.

## 3.2. Numerical analysis of pairwise- and edge-based models

The numerical analysis part focuses around comparisons between the 'original' degree-dependent weighted networks and the two null models. Namely, we consider the network with the same weight distribution but with the weights distributed at random, and the case of all weights equal to the average weight. For all cases we use a network where nodes can be of either a low or high degree, i.e. degrees of two types only. In Fig. 7, we present time evolution plots for the prevalence. There are several important observations that can be made. Firstly, the agreement between the pairwise, edge-based and simulation model is excellent for different parameter values and weight function combinations. Secondly, the distribution of weights has a significant impact on the time evolution of the epidemic with the homogenous/equal link-weight case giving rise to the fastest growing epidemic (see top panel of Fig. 7 for the strongest effect) . The difference between the randomly distributed and equal weights cases is not significant, and both lead to fast epidemics compared to the original network model, where the epidemic is slower but lasts longer. All the features above become less pronounced if either the transmission rate, $\tau$, increases (see the bottom panel of Fig. 7) or if the weights are of different magnitude. Both $w_{ij} = 1/(i+j)^{1/2}$ and $w_{ij} = 1/\ln(i+j)$ produce weights that have higher values when compared to the original $w_{ij} = 1/(i \times j)^{1/2}$ case. This explains the smaller differences in the middle and bottom panel of Fig. 7.



https://doi.org/10.1051/mmnp/20149204 Published online by Cambridge University Press

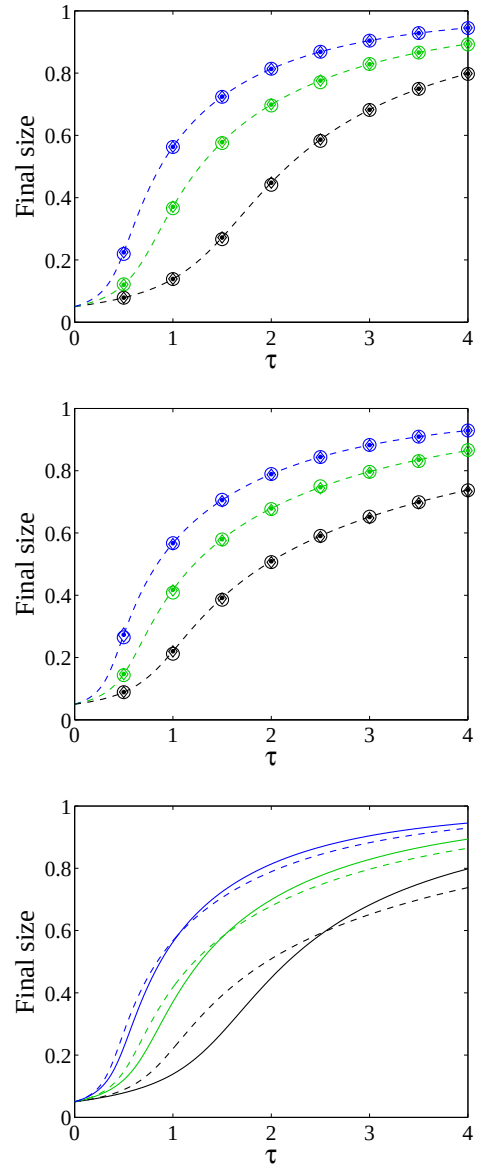



FIGURE 6. Final epidemic size for heterogeneous weighted networks with different weight functions: $w_{ij} = 1/\ln(i+j)$ (blue), $w_{ij} = 1/(i+j)^{1/2}$ (green) and $w_{ij} = 1/(i \times j)^{1/2}$ (black) (or top to bottom in each figure). The dash lines correspond to $R(\infty) = 1 - \psi(\theta(\infty))$ with $\rho = 0.05$ (equivalent to $I_0 = 50$ out of $N = 1000$ in simulations) , $\psi(\theta(\infty))$ corresponds to Eqs. (3.5-3.7) and Eqs. (3.12-3.15) from top to middle panel, respectively. The markers correspond to $\tau = 0.5, 1.0, ..., 4$ for simulation ($\circ$), pairwise ($\diamond$) and edge-based ($\bullet$). All numerical tests use $N = 1000$, $P(l) = 0.8$, $P(h) = 1 - P(l)$, $I_0 = 50$, $l = 3$, $h = 13$ and $\gamma = 1$, and simulations are averaged over 50 different network realisations and 50 simulations on each of these. The top and middle panel represent degree-dependent networks and networks with random weight distribution but with the same average weight as in the degree-dependent case $\langle w \rangle_{dd} = q_1 w_{ll} + q_2 w_{lh} + q_3 w_{hh}$, respectively. The bottom panel is simply the superposition of the top and middle panel, with continuous and dashed lines for degree-dependent and random weights, respectively.



https://doi.org/10.1051/mmnp/20149204 Published online by Cambridge University Press

The marked difference in the time evolution of the epidemics can be explained intuitively by noting that on networks with degree-dependent weights, and especially when weights and degrees are inversely correlated, the important role played by highly connected nodes is negated by small link weights which makes transmission less likely. The slow initial growth in prevalence shows that the epidemic is 'struggling' to infect the highly connected nodes of the network, where link weights are the lowest. The transmission process is mainly capturing nodes that are less well connected with this process being favoured by larger link-weights. This effect fades away as the value of $\tau$ increases.

### 3.3. The principle of formally proving model equivalence

Our numerical results show remarkable agreement between the pairwise and the EBCM models, see Figs. 5-7. A careful analysis (is in a separate publication [25]) shows that while the two models appear to make different assumptions, they are in fact equivalent. We will give some insight into why this occurs. The central observation is that with both models, we will show that when considering two neighbours $u$ and $v$, in our calculation of whether $v$ has infected $u$ it is rigorously possible to ignore whether any other neighbours have previously infected $u$.

The EBCM approach proceeds by starting with the initial problem of calculating the proportion of the population that is in each state. By assuming that the population-scale dynamics are deterministic, we can conclude that this must equal the probability that a random individual is in each state. So we transition to the equivalent problem of choosing a random individual $u$ and calculating its probability of being in a given state. We seek to calculate the probability that a random neighbor $v$ of $u$ has transmitted infection to $u$. This is complicated by the fact that $u$ might first transmit to $v$. However, we note that preventing $u$ from transmitting to $v$ after infection of $u$ does not alter the probability that $u$ is susceptible, infected, or recovered. Thus we find another equivalent problem: to calculate the probability that $u$ is in each state given that it is prevented from transmitting to its partners. This sequence of arguments means that as we calculate whether $v$ has transmitted to $u$, we can ignore whether or not another neighbor has already transmitted to $u$.

In the pairwise model, we look at the equations for the rates of change of $[S_kS_{k'}]$, $[S_kI_{k'}]$, and $[S_kR_{k'}]$ in Eq. (2.3). In each equation, there is a term on the right hand side which represents infection of the $S_k$ individual by a partner other than the $k'$ individual. After substituting our closure relation, each of these terms looks like $-[S_kS_{k'}]f$, $-[S_kI_{k'}]f$, and $-[S_kR_{k'}]f$ where

$$f = -\tau\frac{k-1}{k}\frac{w_{kq}\sum_q[I_qS_k]}{[S_k]} = \frac{k-1}{k}\frac{\dot{[S_k]}}{[S_k]}.$$

So each of equations is of the form $\dot{x} = -xf + y$ where the $y$ terms represent other effects. By moving the $xf$ term to the left hand side, we can use an integrating factor which yields a differential equation for the new variable $xe^F$ where $\dot{F} = f$. The $y$ terms remain in the equation, multiplied by $e^F$, but the term that represented infection of the $S_k$ individual by a partner other than the $k'$ individual has been eliminated. If we follow this change of variables and perform a few more simplifications, it is possible to arrive at the EBCM equations.

## 4. Discussion

In this paper we have shown that the pairwise and edge-based compartmental models can be successfully extended to specific cases of weighted networks and studied the non-trivial case of non-independence between weights and nodal degrees. In particular, we assumed that the link weight is inversely proportional to the degrees of the nodes that it connects. This model has been compared to two null models where for both the network topology remains the same and only the distribution of weights changes. First, we considered the case when the original weights are 'lifted of' the edges and redistributed at random, thus



https://doi.org/10.1051/mmnp/20149204 Published online by Cambridge University Press

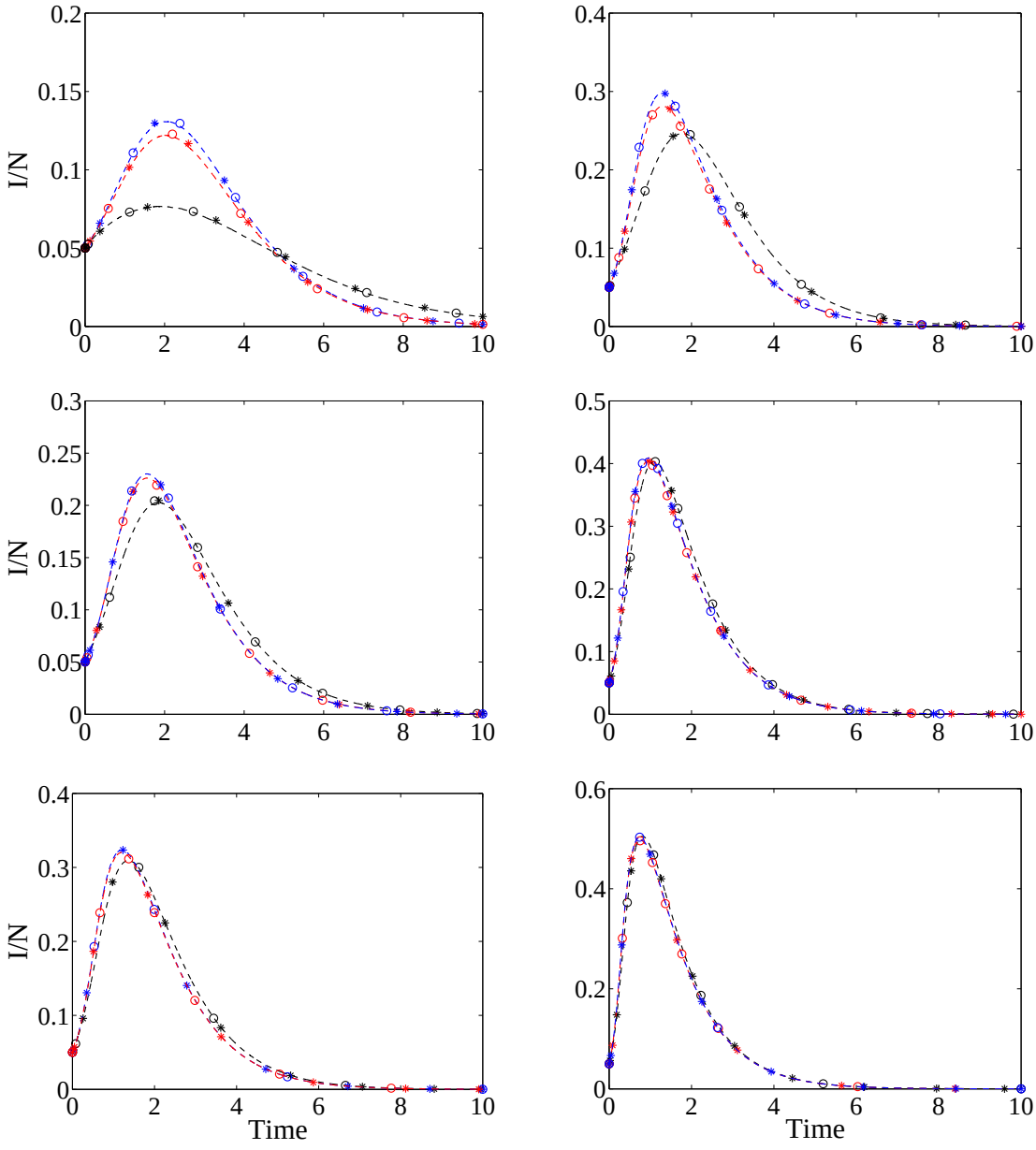



FIGURE 7. The infection prevalence ($I/N$) from heterogeneous weighted networks (simulation: dashed line, pairwise: ($\circ$), and edge-based: ($\star$)). All numerical tests use $N = 1000$, $P(l) = 0.8$, $P(h) = 1 - P(l)$, $I_0 = 50$, $l = 3$, $h = 13$, $\gamma = 1$, and simulations are averaged over 50 different network realisations and 50 simulations on each of these. Degree-dependent weighted networks (black), networks with randomly distributed weights (red) and networks with equal weights (blue). All networks have the same average weight $\langle w \rangle_{dd} = q_1 w_{ll} + q_2 w_{lh} + q_3 w_{hh}$. From top to bottom: $w_{ij} = 1/(i \times j)^{1/2}$, $w_{ij} = 1/(i + j)^{1/2}$ and $w_{ij} = 1/\ln(i + j)$, and left and right with $\tau = 2$ and $\tau = 4$, respectively.



https://doi.org/10.1051/mmnp/20149204 Published online by Cambridge University Press

making weights and nodal degrees independent , and secondly, the networks with all weights equal has been considered.

The results show that the negative correlation between weights and nodal degrees can negate the important role played by highly connected nodes in standard epidemic models on non-weighted graphs, and that weight heterogeneity but with the same overall average or total weight, reduce the value of $R_0$. The relation between final epidemic size and $R_0$, as expected, is determined by the model structure and, in this case, the same $R_0$ value leads to the biggest final epidemic size on degree-dependent weighted networks.

An important by-product of our analysis is the issue around model equivalence. This aspect emerged from the numerical evaluation and comparison of pairwise, edge-based and simulation models. The excellent agreement between all three, but especially, the agreement between pairwise and the edge-based model lead us to consider whether the two models are indeed equivalent. While, here we only present the basic idea of a formal proof, in [25] we will present detailed arguments to show the relationship between these models and other models for SIR epidemics on networks. We believe that in a model 'rich' environment, this part of our study and future work , as well as of others in the community [23], are important in trying to reconcile as much as possible different modelling approaches and to identify model hierarchies, as well as to pinpoint model efficiencies in terms of generating analytical or semi-analytical results.

*Acknowledgements.* P. Rattana acknowledges funding for her Ph.D. studies from the Ministry of Science and Technology, Thailand. JCM was supported in part by: 1) the RAPIDD program of the Science and Technology Directorate, Department of Homeland Security and the Fogarty International Center, National Institutes of Health, and 2) the Center for Communicable Disease Dynamics, Department of Epidemiology, Harvard School of Public Health under Award Number U54GM088558 from the National Institute Of General Medical Sciences. The content is solely the responsibility of the authors and does not necessarily represent the official views of the National Institute Of General Medical Sciences or the National Institutes of Health. We thank Prof Péter L. Simon for pointing out a viable approach to proving that $R_0^{dd} \leq R_0^{rw}$.

## Appendix A: Proof of $R_0^{dd} \leq R_0^{rw}$

We wish to provide a formal proof that $R_0^{dd} \leq R_0^{rw}$. This amounts to showing that

$$R_0^{dd} = \frac{R_1 + R_2 + \sqrt{(R_1 - R_2)^2 + 4F}}{2} \leq ((l-1)P_e(l) + (h-1)P_e(h))\,(q_1 r_1 + q_2 r_2 + q_3 r_3) = R_0^{rw}.$$

We introduce the following notation: $x = P_e(h)$, $y = P_e(l)$. Then $y = 1 - x$ (with both $x, y \in [0,1]$) and

$$q_1 = y^2,\ q_2 = 2xy,\ q_3 = x^2,\ a = (h-1)xr_3,\ b = (l-1)yr_1,\ d = 1 - \frac{r_2^2}{r_1 r_3}.$$

We will make use of the following straightforward inequalities:

1. $r_3 \leq r_2 \leq r_1$,
2. $d \leq 0 \leftrightarrow r_1 r_3 \leq r_2^2$,
3. $(h-1)r_3 \geq (l-1)r_1$.

We also note that $r_3 \leq r_2$ implies that $(h-1)r_2 \geq (h-1)r_3 \geq (l-1)r_1$. These can be simply checked and formally proven by plugging in the corresponding expressions and performing some standard algebraic manipulation to reach some equivalent inequalities that trivially hold.

The l.h.s. of the inequality is the positive root of the quadratic polynomial

$$\lambda^2 - \lambda(a+b) + abd = 0,$$



https://doi.org/10.1051/mmnp/20149204 Published online by Cambridge University Press

where $abd \leq 0$, since $d$ is negative while $a$ and $b$ are positive. Hence, the roots of this polynomial are denoted by $\lambda_2 < 0 < \lambda_1$. Then the following has to be proved,

$$\lambda_1 \leq [(h-1)x + (l-1)y](x^2 r_3 + 2xyr_2 + y^2 r_1).$$

First we give an upper estimate of $\lambda_1$. Using the formula for $\lambda_1$ and the inequality $\sqrt{1+x} \leq 1 + x/2$, one obtains

$$\lambda_1 = \frac{a+b+\sqrt{(a+b)^2 - 4abd}}{2} = \frac{a+b+(a+b)\sqrt{1-4abd/(a+b)^2}}{2} \leq a+b-\frac{abd}{a+b}.$$

It is also easy to show that $a+b \geq (l-1)r_1$. This can be done by considering $a+b = (h-1)r_3 x + (l-1)(1-x)r_1 = [(h-1)r_3 - (l-1)r_1]x + (l-1)r_1$ as a function of $x$. Due to $(h-1)r_3 \geq (l-1)r_1$, the function above is monotone increasing, and since $x \in [0,1]$, the function will attain its minimum at $x = 0$, and the minimum is $(l-1)r_1$. Using this in the inequality for $\lambda_1$ yields

$$\lambda_1 \leq a+b-\frac{abd}{a+b} \leq a+b-\frac{abd}{(l-1)r_1}.$$

Thus it is enough to prove that

$$a+b-\frac{abd}{(l-1)r_1} \leq [(h-1)x + (l-1)y](x^2 r_3 + 2xyr_2 + y^2 r_1).$$

Let the difference of the l.h.s and the r.h.s be

$$f(x) = [(h-1)x + (l-1)y](x^2 r_3 + 2xyr_2 + y^2 r_1) - (h-1)xr_3 - (l-1)yr_1 + d(h-1)r_3 xy.$$

Then it is enough to prove that for all $x \in [0,1]$ we have $f(x) \geq 0$. Since $y = 1-x$, it is easy to see that $f(x)$ is a cubic polynomial and $f(0) = 0$, $f(1) = 0$. Hence, it is enough to prove that $f'(0) > 0$ and $f'(1) < 0$. Simple algebra shows that

$$r_1 f'(0) = (r_1 - r_2)\{r_1(h-l) + [(h-1)r_2 - (l-1)r_1]\} \geq 0,$$

based on that $r_1 \geq r_2$, $l \leq h$ and $(h-1)r_2 \geq (l-1)r_1$. The inequality $f'(1)$ develops as follows,

$$r_1 f'(1) = (l-1)r_1(r_1 - r_3) + (h-1)(r_2^2 - 2r_2 r_1 + r_1 r_3) \leq (h-1)r_3(r_1 - r_3) + (h-1)(r_2^2 - 2r_2 r_1 + r_1 r_3),$$

and this can be rearranged to give

$$r_1 f'(1) \leq (h-1)(r_2 - r_3)(r_2 + r_3 - 2r_1) \leq 0,$$

since $r_3 \leq r_2 \leq r_1$. Thus the original inequality holds.

## Appendix B : Proof of the invariance of the final size and $R_0$ relation

First, let us consider the final epidemic size corresponding to networks with random weight distribution

$$R^{rw}(\infty) = 1 - (1-\rho)(P(l)\theta_{rw}^l(\infty) + P(h)\theta_{rw}^h(\infty)), \tag{B.1}$$

where $\theta_{rw}(\infty) = q_1\theta_{w_1}(\infty) + q_2\theta_{w_2}(\infty) + q_3\theta_{w_3}(\infty)$. Substituting Eqs. (3.5-3.7) into $\theta_{rw}(\infty)$ and using Eq. (3.4), we have

$$\theta_{rw}(\infty) = q_1 \frac{\gamma + (1-\rho)\tau_{rw}\ w_1\left[P_e(l)\theta_{rw}^{l-1}(\infty) + P_e(h)\theta_{rw}^{h-1}(\infty)\right]}{\tau_{rw} w_1 + \gamma}$$



https://doi.org/10.1051/mmnp/20149204 Published online by Cambridge University Press

$$+ q_2 \frac{\gamma + (1-\rho)\tau_{rw} w_2 \left[P_e(l)\theta_{rw}^{l-1}(\infty) + P_e(h)\theta_{rw}^{h-1}(\infty)\right]}{\tau_{rw} w_2 + \gamma}$$
$$+ q_3 \frac{\gamma + (1-\rho)\tau_{rw} w_3 \left[P_e(l)\theta_{rw}^{l-1}(\infty) + P_e(h)\theta_{rw}^{h-1}(\infty)\right]}{\tau_{rw} w_3 + \gamma}$$
$$= \frac{\zeta - R_0^{rw}}{\zeta} + \frac{R_0^{rw}}{\zeta}(1-\rho)\left[P_e(l)\theta_{rw}^{l-1}(\infty) + P_e(h)\theta_{rw}^{h-1}(\infty)\right]. \tag{B.2}$$

Next, the final epidemic size corresponding to networks with all weights equal to the average weight is

$$R^{av}(\infty) = 1 - (1-\rho)(P(l)\theta_{av}^{l}(\infty) + P(h)\theta_{av}^{h}(\infty)). \tag{B.3}$$

Similarly, based on Eqs. (2.4-2.5) and Eq. (3.16), and using that the average weight $w_{av} = \langle w \rangle_{dd} = q_1 w_1 + q_2 w_2 + q_3 w_3$, $\theta_{av}(\infty)$ can be writhen as,

$$\theta_{av}(\infty) = \frac{\gamma + (1-\rho)\tau_{av}(q_1 w_1 + q_2 w_2 + q_3 w_3)\left[P_e(l)\theta_{av}^{l-1}(\infty) + P_e(h)\theta_{av}^{h-1}(\infty)\right]}{\tau_{av}(q_1 w_1 + q_2 w_2 + q_3 w_3) + \gamma}$$
$$= \frac{\zeta - R_0^{av}}{\zeta} + \frac{R_0^{av}}{\zeta}(1-\rho)\left[P_e(l)\theta_{av}^{l-1}(\infty) + P_e(h)\theta_{av}^{h-1}(\infty)\right]. \tag{B.4}$$

Now, we start by assuming that $R^{rw}(\infty) = R^{av}(\infty)$, then Eqs. (B.1) & (B.3) lead to

$$\theta_{rw}(\infty) = \theta_{av}(\infty) = \theta \tag{B.5}$$

due to the function $f(x) = ax^l + bx^h$ being strictly monotonically increasing on our domain of interest $x \in [0,1]$, and beyond. Using Eq. (B.5) and Eqs. (B.2) & (B.4) yields

$$\frac{\zeta - R_0^{av}}{\zeta} + \frac{R_0^{av}}{\zeta}(1-\rho)\left[P_e(l)\theta^{l-1} + P_e(h)\theta^{h-1}\right] = \frac{\zeta - R_0^{rw}}{\zeta} + \frac{R_0^{rw}}{\zeta}(1-\rho)\left[P_e(l)\theta^{l-1} + P_e(h)\theta^{h-1}\right],$$

$$(R_0^{av} - R_0^{rw})\left(1 - (1-\rho)\left[P_e(l)\theta^{l-1} + P_e(h)\theta^{h-1}\right]\right) = 0,$$
$$R_0^{av} = R_0^{rw}.$$

## References


[1] D.A. Rand. *Correlation equations and pair approximations for spatial ecologies.* CWI Quarterly., 12 (1999), 329–368.

[2] D.T. Gillespie. *Exact stochastic simulation of coupled chemical reactions.* J. Phys. Chem., 81 (1977), 2340–2361.

[3] F. Ball, P. Neal. *Network epidemic models with two levels of mixing.* Math. Biosci., 212 (2008), 69–87.

[4] J.C. Miller. *Epidemics on networks with large initial conditions or changing structure.* Available at http://arxiv.org/abs/1208.3438.

[5] J.C. Miller. *Spread of infectious disease through clustered populations.* J. Roy. Soc. Interface., 6 (2009), 1121–1134.

[6] J.C. Miller, A.C. Slim, E.M. Volz. *Edge-based compartmental modelling for infectious disease spread.* J. Roy. Soc. Interface., 9 (2012), 890–906.

[7] J.C. Miller, E.M. Volz. *Edge-based compartmental modeling with disease and population structure.* Available at http://arxiv.org/abs/1106.6344.

[8] J. Joo, J.L. Lebowitz. *Behavior of susceptible-infected-susceptible epidemics on heterogeneous networks with saturation.* Phys. Rev. E., 69 (2004), 066105.

[9] J. Lindquist, J. Ma, P. Van den Driessche, F.H. Willeboordse. *Effective degree network disease models.* J. Math. Biol., 62 (2011), 143–164.

[10] K.B. Athreya, P.E. Ney, Branching processes. Dover Publications, Inc., Mineola, New York, 2008.

[11] K.J. Sharkey, C. Fernandez, K.L. Morgan, E. Peeler, M. Thrush, J.F. Turnbull, R.G. Bowers. *Pair-level approximations to the spatio-temporal dynamics of epidemics on asymmetric contact networks.* J. Math. Biol., 53 (2006), 61–85.

[12] K.T.D. Eames. *Modelling disease spread through random and regular contacts in clustered populations.* Theor. Popul. Biol., 73 (2008), 104–111.

[13] K.T.D. Eames, J.M. Read, W.J. Edmunds, *Epidemic prediction and control in weighted networks.* Epidemics., 1 (2009), 70–76.




https://doi.org/10.1051/mmnp/20149204 Published online by Cambridge University Press

[14] K.T.D. Eames, M.J. Keeling. *Modeling dynamic and network heterogeneities in the spread of sexually transmitted diseases.* Proc. Natl. Acad. Sci. USA., 99 (2002), 13330–13335.

[15] M. Deijfen. *Epidemics and vaccination on weighted graphs.* Math. Biosci., 232 (2011), 57–65.

[16] M.E.J. Newman. *Spread of epidemic disease on networks.* Phys. Rev. E., 66 (2002), 016128.

[17] M. Gilbert, A. Mitchell, D. Bourn, J. Mawdsley, R. Clifton-Hadley, W. Wint. *Cattle movements and bovine tuberculosis in Great Britain.* Nature., 435 (2005), 491–496.

[18] M.J. Keeling. *The effects of local spatial structure on epidemiological invasions.* Proc. R. Soc. Lond. B., 266 (1999), 859–867.

[19] M. Molloy, B. Reed. *A critical point for random graphs with a given degree sequence.* Random Struct Alg., 6 (1995), 161–180.

[20] P. Rattana, K.B. Blyuss, K.T.D. Eames, I.Z. Kiss. *A class of pairwise models for epidemic dynamics on weighted networks.* Accepted for publication in Bull. Math. Biol., (2012).

[21] R. Olinky, L. Stone. *Unexpected epidemic thresholds in heterogeneous networks: The role of disease transmission.* Phys. Rev. E., 70 (2004), 030902(R).

[22] T. Britton, M. Deijfen, F. Liljeros. *A weighted configuration model and inhomogeneous epidemics.* J. Stat. Phys., 145 (2011), 1368-1384.

[23] T. House, M.J. Keeling. *Insights from unifying modern approximations to infections on networks.* J. Roy. Soc. Interface., 8 (2011), 67–73.

[24] V. Marceau, P-A. Noël, L. Hébert-Dufresne, A. Allard, L.J. Dubé. *Adaptive networks: coevolution of disease and topology.* Phys. Rev. E., 82 (2010), 036116.

[25] J. C. Miller, I. Z. Kiss. *Epidemic Spread in Networks: Existing Methods and Current Challenges*, Math. Model. Nat. Phenom. Vol. 9, No. 2, (2014), 4–42.



https://doi.org/10.1051/mmnp/20149204 Published online by Cambridge University Press